Langmuir
Article
pubs.acs.org/Langmuir

Revealing the Lytic Mechanism of the Antimicrobial Peptide Gomesin by Observing Giant Unilamellar Vesicles

Tatiana M. Domingues, Karin A. Riske,* and Antonio Miranda*

Departamento de Biofísica, Universidade Federal de São Paulo, R. Três de Maio, 100 CEP 04044-020, São Paulo, SP, Brazil

Received February 12, 2010. Revised Manuscript Received March 9, 2010

Gomesin (Gm) is a potent cationic antimicrobial peptide from a Brazilian spider. Here we use optical and fluorescence microscopy to study the interaction of Gm, its low active linear analogue, [Ser^{2,6,11,15}]-Gm (GmL), and a fluorescent labeled analogue, Gm-Rh, with giant unilamellar vesicles (GUVs) composed of mixtures of the neutral lipid palmitoyloleoyl phosphatidylcholine (POPC) with the negatively charged lipid palmitoyloleoyl phosphatidylglycerol (POPG) or cholesterol, so as to mimic bacterial and mammalian cell membranes, respectively. We observed the effect of injecting a peptide solution with a micropipet close to GUVs. As a result of peptide−lipid interaction, GUVs burst suddenly. Stable pores, which result in leaky vesicles, were not observed. Fluorescence microscopy of Gm-Rh injected on GUVs confirmed the high peptide/lipid affinity. These facts lead us to suggest that Gm and GmL disrupt the membrane via the carpet model. In order to quantify the lytic activity of both peptides against different membrane composition, a solution of GUVs was diluted in increasing concentration of peptides and the fraction of burst GUVs was measured as a function of time. The lytic activity of both peptides was enhanced by the presence of POPG and decreased upon addition of cholesterol. GmL exhibited lower lytic activity as compared to Gm, but this difference vanished at high POPG molar fraction.

Introduction

Antimicrobial peptides (AMPs) play an important role in the innate immune defense system of animals and plants.[1−3] In fact, innumerous organisms use AMPs against bacteria, fungi, and other pathogenic agents.[4,5] These types of molecules are essential components of strategic and well regulated mechanisms of immunity to infection; in addition, they generally display a minimal toxicity against mammalian cells.[6,7] There is an increasing interest in the pharmacological application of AMPs mainly due to the growing problem of pathogenic organisms resistant to conventional antibiotics.[8] The majority of these peptides share some common features, such as low molecular weight (less than 5 kDa), positive net charge at physiological pH, and amphipathic character.[9] Among them, the cysteine-rich family has been largely investigated in the past years,[10] since the maintenance of at least one intramolecular disulfide bridge seems to be fundamental to maintain the antimicrobial activity.[11,12]

Gomesin (Gm) is a potent AMP that was isolated and characterized from hemocytes of the Brazilian spider *Acanthoscurria gomesiana*.[13] The peptide contains 18 amino acid residues (ZCRRLCYKQRCVTYCRGR-NH_2, Z = pGlu), including 6 cationic residues and 4 cysteines that form two disulfide bridges: Cys$^{2-15}$ and Cys$^{6-11}$. It contains a pyroglutamic acid (Z) at the N-terminus and is amidated at the C-terminus. These features certainly contribute to the stability of the Gm molecule to proteases within the hemocytes.[14] Previous studies showed that Gm adopts a β-hairpin structure in aqueous solution.[15] Gm is very effective against several bacteria, fungi and parasites.[13,16−18] Antitumor activity of Gm was also confirmed in vitro and in vivo.[19,20] Due to its large range of antimicrobial activity, Gm seems to be a very good lead compound in the development of new drugs for human therapy.[13,21] Although Gm exhibits hemolytic activity against human erythrocytes, this activity could be significantly reduced through modifications in the Gm molecular structure.[22] The linear analogue [Ser^{2,6,11,15}]-Gm (GmL) has the Cys residues

*To whom correspondence should be addressed. Telephone: +55 11-5539-0809. Fax: +55 11-5575-9617. E-mail: kariske@unifesp.br (K.A.R.); amiranda@unifesp.br (A.M.).

(1) Jenssen, H.; Hamill, P.; Hancock, R. E. *Clin. Microbiol. Rev.* **2006**, *19*, 491–511.
(2) Giuliani, A.; Pirri, G.; Nicoletto, S. F. *Cent. Eur. J. Biol.* **2007**, *2*, 1–33.
(3) Brogden, K. A.; Ackermann, M.; McCray, P. B., Jr.; Tack, B. F. *Int. J. Antimicrob. Agents* **2003**, *22*, 465–478.
(4) Bulet, P.; Stocklin, R.; Menin, L. *Immunol. Rev.* **2004**, *198*, 169–184.
(5) Zasloff, M. *Nature* **2002**, *415*, 389–395.
(6) Blazyk, J.; Wiegand, R.; Klein, J.; Hammer, J.; Epand, R. M.; Epand, R. F.; Maloy, W. L.; Kari, U. P. *J. Biol. Chem.* **2001**, *276*, 27899–27906.
(7) Dathe, M.; Meyer, J.; Beyermann, M.; Maul, B.; Hoischen, C.; Bienert, M. *Biochim. Biophys. Acta* **2002**, *1558*, 171–186.
(8) Yeaman, M. R.; Yount, N. Y. *Pharmacol. Rev.* **2003**, *55*, 27–55.
(9) Toke, O. *Biopolymers* **2005**, *80*, 717–735.
(10) Dimarcq, J. L.; Bulet, P.; Hetru, C.; Hoffmann, J. *Biopolymers* **1998**, *47*, 465–477.
(11) Bulet, P.; Hetru, C.; Dimarcq, J. L.; Hoffmann, D. *Dev. Comp. Immunol.* **1999**, *23*, 329–344.
(12) Fazio, M. A.; Oliveira, V. X., Jr.; Bulet, P.; Miranda, M. T.; Daffre, S.; Miranda, A. *Biopolymers* **2006**, *84*, 205–218.
(13) Silva, P. I., Jr.; Daffre, S.; Bulet, P. *J. Biol. Chem.* **2000**, *275*, 33464–33470.
(14) Moraes, L. G.; Fazio, M. A.; Vieira, R. F.; Nakaie, C. R.; Miranda, M. T.; Schreier, S.; Daffre, S.; Miranda, A. *Biochim. Biophys. Acta* **2007**, *1768*, 52–58.
(15) Mandard, N.; Bulet, P.; Caille, A.; Daffre, S.; Vovelle, F. *Eur. J. Biochem.* **2002**, *269*, 1190–1198.
(16) Sacramento, R. S.; Martins, R. M.; Miranda, A.; Dobroff, A. S.; Daffre, S.; Foronda, A. S.; De Freitas, D.; Schenkman, S. *Parasitology* **2009**, *136*, 813–821.
(17) Moreira, C. K.; Rodrigues, F. G.; Ghosh, A.; Varotti Fde, P.; Miranda, A.; Daffre, S.; Jacobs-Lorena, M.; Moreira, L. A. *Exp. Parasitol.* **2007**, *116*, 346–353.
(18) Barbosa, F. M.; Daffre, S.; Maldonado, R. A.; Miranda, A.; Nimrichter, L.; Rodrigues, M. L. *FEMS Microbiol. Lett.* **2007**, *274*, 279–286.
(19) Rodrigues, E. G.; Dobroff, A. S.; Taborda, C. P.; Travassos, L. R. *An. Acad. Bras. Cienc.* **2009**, *81*, 503–520.
(20) Rodrigues, E. G.; Dobroff, A. S.; Cavarsan, C. F.; Paschoalin, T.; Nimrichter, L.; Mortara, R. A.; Santos, E. L.; Fazio, M. A.; Miranda, A.; Daffre, S.; Travassos, L. R. *Neoplasia* **2008**, *10*, 61–68.
(21) Miranda, A.; Miranda, M. T. M.; Jouvensal, L.; Vovelle, F.; Bulet, P.; Daffre, S. *A powerful antimicrobial peptide isolated from the brazilian tarantula spider Acanthuscurria gomesiana*; Editora UFMG: Belo Horizonte, 2009; pp 323−343.
(22) Fazio, M. A.; Jouvensal, L.; Vovelle, F.; Bulet, P.; Miranda, M. T.; Daffre, S.; Miranda, A. *Biopolymers* **2007**, *88*, 386–400.

replaced by Ser, and therefore, the disulfide bridges are absent. Consequently, GmL assumes a random structure in aqueous solution but acquires a β-hairpin-like structure in the presence of sodium dodecyl sulfate (SDS) micelles.[12] The antimicrobial and hemolytic activities of GmL are significantly lower than those of Gm, showing that peptide structure is essential to its activity.[22]

Putative mechanisms of the antimicrobial action of Gm and other AMPs involve membrane permeabilization, mainly via a nonspecific interaction with the lipid phase.[2,4,12,15,23−25] On the one hand, positively charged AMPs accumulate at the membrane surface of microorganisms, rich in the negatively charged lipid PG (phosphatidylglycerol). On the other hand, the amphiphilic character of the AMPs facilitates their insertion into lipid bilayers with subsequent formation of pores and/or disruption of membranes. Thus, the interaction of AMPs with lipid bilayers and micellar systems of controlled compositions has been extensively studied as a means to gain knowledge on the not yet fully understood mechanism of membrane destabilization by AMPs.[14,22,26] In particular, giant unilamellar vesicles (GUVs, diameter around 10 μm) have been used recently in such studies because their morphology and dynamics can be directly followed with more detail by using optical microscopy.[25,27−30] One advantage of GUVs over the most commonly used large unilamellar vesicles (LUVs, with 100 nm diameter) is the possibility of distinguishing among different mechanisms of membrane destabilization through optical observation of a single GUV in the presence of AMPs. Ambroggio et al. were the first to suggest that gradual leakage of GUVs was characteristic of toroidal pore formation, whereas abrupt GUV bursting was an indication of the carpet mechanism.[30] Furthermore, they rationalized their observation with different AMPs based on their effective length. Only peptides long enough to span the bilayer would be able to form stable pores. Tamba and co-workers showed that magainin 2, one of the most studied AMPs, induces the opening of stable pores in GUVs, followed by the slow release of their inner content.[29] On the other hand, another AMP, the tea catechin EGCg, causes sudden burst of the GUVs with instantaneous release of the entrapped volume.[28] This led them to propose that magainin 2 acts indeed via the toroidal pore model, whereas tea catechin disrupts the bilayer through the carpeting mechanism.

In this work, we use optical microscopy of GUVs to gain new insights into the lytic mechanism of Gm and one of its linear analogues, GmL. The GUVs were made of different molar fractions of the neutral lipid palmitoyloleoyl phosphatidylcholine (POPC) and the negatively charged lipid palmitoyloleoyl phosphatidylglycerol (POPG), with the aim of mimicking the composition of bacterial membranes. For comparison, GUVs of POPC with 40 mol % cholesterol were used as a model membrane of mammalian cells. First, a solution of Gm or GmL was injected close to single GUVs with the aim of qualitatively describing the general lytic mechanism of the peptides. We also use fluorescence microscopy to follow the injection of a fluorescently labeled Gm. As far as we know, this is the first work to track a fluorescently labeled AMP during its activity against GUVs. In another setup, GUVs of different membrane compositions were diluted in a solution containing increasing concentrations of either Gm or GmL and the number of GUVs as a function of time was counted. This allowed us to quantify the lytic activity of both peptides against membrane with different composition.

Materials and Methods

Materials. POPC (1-palmitoyl-2-oleoyl-*sn*-glycero-3-phosphocholine), POPG (1-palmitoyl-2-oleoyl-*sn*-glycero-3-[phospho-rac-(1-glycerol)]), and cholesterol were purchased from Avanti Polar Lipids (Birmingham, AL) and were used without further purification. Rhodamine [5(6)-carboxytetramethylrhodamine *N*-succinimidyl ester] was acquired from Sigma-Aldrich (St. Louis, MO). $DiIC_{18}$ (1,19-dioctadecyl-3,3,39,39-tetramethylindocarbocyanine perchlorate) was purchased from Molecular Probes (Eugene, OR).

Peptide Synthesis. Peptides were synthesized manually by the solid-phase method on a 4-methylbenzhydrylamine-resin (MBHAR) (0.8 mmol/g) using the *t*-Boc strategy.[12] Full deprotection and cleavage of the peptide from the resin were carried out using anhydrous HF treatment with anisole and dimethyl sulfide (DMS) as scavengers at 0 °C for 1.5 h. Formation of disulfide bridges was achieved immediately after the HF cleavage and extraction of the crude peptide. The resulting peptide solution was kept at pH 6.8−7.0 and 5 °C for 72 h. Cyclization reactions were monitored by reverse-phase liquid chromatography coupled to an electrospray ionization mass spectrometer (LC/ESI-MS). Lyophilized crude peptides were purified by preparative RP-HPLC on a column Vydac C_{18} (25 × 250 mm, 300 Å pore size, 15 μm particle size) in two steps. The first was performed by using triethylammonium phosphate (TEAP) pH 2.25 as solvent A and 60% acetonitrile (ACN) in A as solvent B. The second step was carried out using 0.1% trifluoroacetic acid (TFA) H_2O as solvent A and 60% ACN in A as solvent B. Pure peptides were characterized by amino acid analysis and by LC/ESI-MS.

Peptides were fluorescently labeled by addition of rhodamine to the Lys side chain as follows: 5 mg of the purified peptides, 2 mg of 5(6)-carboxytetramethylrhodamine *N*-succinimidyl ester, and 4 μL of DIPEA (*N*,*N*-diisopropylethylamine) in 500 μL of DMF (*N*,*N*-dimethylformamide) were kept for 2 h at room temperature. The resulting labeled peptides were repurified by preparative RP-HPLC using 0.1% TFA/H_2O as solvent A and 60% ACN in A as solvent B. Pure peptides were also characterized by LC/ESI-MS.

Preparation and Observation of Giant Unilamellar Vesicles (GUVs). Giant unilamellar vesicles made of mixtures of POPC with either POPG or cholesterol were grown using the electroformation method.[31] Briefly, 10 μL of a 2 mg/mL lipid chloroform solution was spread on the surfaces of two conductive glasses (coated with fluorine tin oxide) and were left under vacuum for ~2 h to remove all traces of the organic solvent. The glasses were placed with their conductive sides facing each other and separated by a 2 mm thick Teflon frame to form a chamber which was filled with 0.2 M sucrose solution. The glass plates were connected to a function generator, and an alternating current of 1 V with a 10 Hz frequency was applied for about 2 h. Before observation, the vesicle solution was diluted ~10 times into a 0.2 M glucose solution to create a sugar asymmetry between the inside and the outside of the vesicles. The osmolarities of the sucrose and glucose solutions were measured with a cryoscopic osmometer Osmomat Gonotec 030 (Berlin, Germany) and carefully matched to avoid osmotic pressure effects. Due to the differences in density and refractive index between the sucrose and glucose solutions, the vesicles were stabilized by gravity at the bottom of the observation chamber and had better contrast when observed with phase contrast microscopy.

GUVs were observed with an inverted microscope Zeiss Axiovert 200 (Jena, Germany) equipped with a Zeiss AxioCam HSm

(23) Mandard, N.; Sy, D.; Maufrais, C.; Bonmatin, J. M.; Bulet, P.; Hetru, C.; Vovelle, F. *J. Biomol. Struct. Dyn.* **1999**, *17*, 367–380.
(24) Matsuzaki, K. *Biochim. Biophys. Acta* **1999**, *1462*, 1–10.
(25) Tamba, Y.; Yamazaki, M. *J. Phys. Chem. B* **2009**, *113*, 4846–4852.
(26) Matsuzaki, K.; Sugishita, K.; Ishibe, N.; Ueha, M.; Nakata, S.; Miyajima, K.; Epand, R. M. *Biochemistry* **1998**, *37*, 11856–11863.
(27) Lee, M. T.; Hung, W. C.; Chen, F. Y.; Huang, H. W. *Proc. Natl. Acad. Sci. U.S.A.* **2008**, *105*, 5087–5092.
(28) Tamba, Y.; Ohba, S.; Kubota, M.; Yoshioka, H.; Yoshioka, H.; Yamazaki, M. *Biophys. J.* **2007**, *92*, 3178–3194.
(29) Tamba, Y.; Yamazaki, M. *Biochemistry* **2005**, *44*, 15823–15833.
(30) Ambroggio, E. E.; Separovic, F.; Bowie, J. H.; Fidelio, G. D.; Bagatolli, L. A. *Biophys. J.* **2005**, *89*, 1874–1881.
(31) Angelova, M. I.; Dimitrov, D. S. *Faraday Discuss.* **1986**, *81*, 303–311.

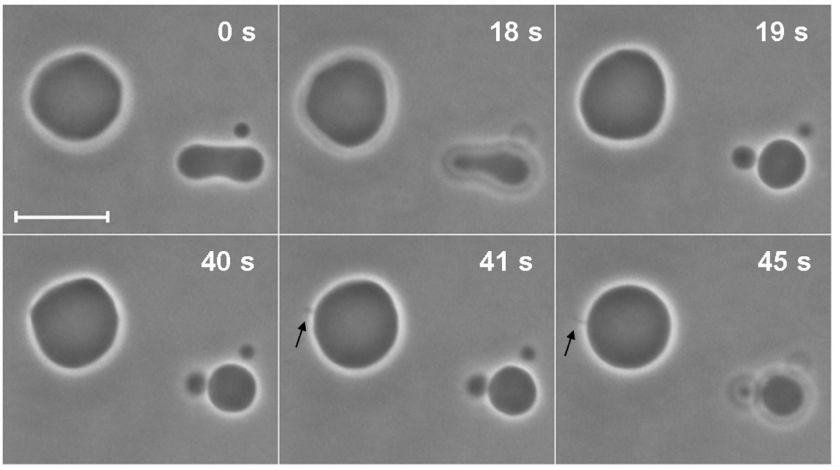

Figure 1. Phase-contrast images showing the shape changes of two GUVs made of POPC/POPG 1:1 induced by injection of a 10 μM solution of Gm with a micropipet. The time shown on top is relative to the moment when the micropipet was brought close to the vesicle (from the right side). The scale bar represents 20 μm. The arrows in snapshots at 41 and 45 s indicate the formation of several buds, like a pearl chain.

digital camera (Jena, Germany). Two different experimental setups were used. In the first one, a 0.2 M glucose solution containing 1−100 μM peptide (Gm, GmL, Gm-Rh, or GmL-Rh) was injected with a glass micropipet of about 15 μm diameter placed at about 50 μm from a chosen GUV. The micropipets were prepared using a vertical puller PC-10 from Narishige (Tokyo, Japan) and were controlled with a micromanipulator MP-225 from Sutter Instruments (Novato, CA). The injection flux was adjusted manually with a micrometer knob pressing a 10 μL Hamilton syringe (Sutter Instruments, Novato, CA). In this setup, the vesicles were observed with a 63× Ph2 objective, either with phase contrast or in fluorescent mode (illumination with a mercury lamp HBO 103 W and a set of filters with excitation at 540−552 nm and emission band of 575−640 nm). In the other experimental setup, 100 μL of a solution of GUVs prepared in 0.2 M sucrose was diluted in 700 μL of a 0.2 M glucose solution containing increasing concentrations of Gm or GmL. The solution was then immediately placed in the observation chamber and followed under phase contrast with a 10× Ph1 objective. A representative observation field (750 × 1000 μm^2) was chosen and recorded for 15 min. The number of GUVs as a function of time for each vesicle composition and each peptide concentration was used as a means to quantify the lytic effect of both peptides. The GUVs were counted manually, and only vesicles bigger than ∼5 μm were chosen. All experiments were performed at room temperature.

Results

The lytic activity of Gm and GmL against giant unilamellar vesicles (GUVs) was evaluated by optical microscopy with two different approaches, which will be presented consecutively. First, single GUVs were followed during micropipet injection of a peptide solution. Alternatively, the injection of a fluorescently labeled Gm (Gm-Rh) close to nonlabeled GUVs was followed with fluorescence microscopy. Second, GUVs made of different membrane compositions were diluted in increasing peptide concentration, and the extent of bursting of an ensemble of GUVs as a function of time was used to quantify the lytic activity of both peptides.

Injection of a Peptide Solution on Single GUVs. In this experimental setup, a micropipet loaded with a peptide solution was brought close to a particular GUV and the injection was started. The flux coming out of the micropipet was somewhat unsteady, and the effective peptide concentration close to the GUVs could not be estimated. The peptide solution loaded in the micropipet ranged from 1 to 100 μM. In this section, we will focus more on the lytic mechanism, in a qualitative manner, and not much on the quantification of the lytic activity, which will be the topic of the following section. Qualitatively, the effects observed were rather independent of membrane composition (pure POPC or POPC/POPG 1:1 mol/mol) and peptide used; they reflect the general mechanism of membrane disruption caused by Gm and its linear analogue GmL. Here, we will concentrate on injections of Gm and its fluorescent analogue, Gm-Rh, for which more experiments were done. Similar results were obtained with GmL and GmL-Rh, although they resulted in lower lytic activity, especially against pure POPC vesicles. The trends described below were observed for at least 50 GUVs for each condition studied.

Noticeable effects on GUVs of POPC/POPG 1:1 were only seen for peptide concentration in the micropipet above 10 μM, whereas at least 50 μM was needed to induce changes in pure POPC vesicles. This indicates that the effective concentration reaching the vesicles is typically 10 times lower, as will become evident in the following section.

All GUVs subjected to injection of at least 50 μM peptide eventually burst, in a stochastic way. Quite often, final vesicle burst was preceded by the formation of small high-contrast domains on the vesicle surface. If a floppy vesicle was chosen, that is, with some excess area, seen by thermal fluctuations of its shape, the injection initially caused a morphological transition to shapes with higher spontaneous curvature, for example, formation of buds. After this initial step, these GUVs also burst. Until final vesicle burst, the GUVs maintained their optical contrast due to sucrose/glucose asymmetry, implying that stable pores were not formed. We will now show some illustrative examples of injection of a peptide solution close to GUVs.

Figure 1 shows a sequence of images of two GUVs with some excess area during the beginning of injection of Gm, before the event of bursting. The vesicle on the right is initially prolate, whereas the other is quasi-spherical or slightly oblate (note that only the equatorial plane is accessible with conventional optical microscopy). The first effect of peptide injection is a morphological change induced by an increase in the membrane spontaneous curvature: First the prolate vesicle undergoes the budding transition, that is, a small vesicle is expelled from the mother vesicle, but both remain connected by a thin neck (snapshots at 18 and 19 s), and afterward the other vesicle also expels several small buds, forming a pearl chain (indicated by arrows in snapshots at

41 and 45 s). The shape of a fluid vesicle at equilibrium is determined by its excess area and its spontaneous curvature.[32] The former parameter depends on the ratio between the effective volume of the vesicle and the volume of a sphere with the same area, whereas the latter accounts for any area difference between the inner and outer monolayers. When molecules adsorb onto the external vesicle surface, this is generally accompanied by an expansion of the outer monolayer without changes in the inner monolayer; consequently, the spontaneous curvature of the bilayer increases.[33−35] Therefore, the increase in spontaneous curvature observed after injection of peptide shows that at this point the peptides adsorb onto the external surface, probably with a shallow penetration in the bilayer from the outside. However, the integrity of the bilayer is preserved, since the optical contrast, due to the sucrose/glucose asymmetry across the bilayer, is maintained. This increase in spontaneous curvature was observed for all GUVs which had some excess area. Such initial superficial interaction was also observed for other AMPs, such as melittin,[36] magainin 2,[29] and the tea catechin EGCg,[28] and shown to be reversible.[28,34] For injections of sufficiently high peptide concentration (> 10−50 μM Gm, depending on the membrane surface charge), the vesicles eventually burst after these morphological changes.

Figure 2 shows three sequences of the bursting of different GUVs caused by injection of Gm, obtained with phase-contrast or fluorescence microscopy of a membrane probe, $DiIC_{18}$. All these vesicles were initially spherical and could be under some initial tension. Panel A shows a time series obtained with phase contrast at our highest recording speed. Within 20 ms, a large hole opens on one side of the vesicle (11.02 s, not in focus). In less than 1 s, the bilayer is disrupted and reduced to a cluster of thin structures, which resemble tubules. Panel B illustrates a vesicle bursting visualized with fluorescence microscopy. Similar to the other example, a large hole suddenly opens on one side of the GUV (3.1 s). The observation in fluorescence mode allows a better image definition. Also, in this particular example, the vesicle bursting was somewhat slower. On the borders of the pore, thin filaments can be seen, which grow as the vesicle disintegrates. Panel C shows another example of vesicle burst. Here we want to call attention to the formation of the high-contrast domains which generally precede vesicle burst. The first snapshot shows a phase-contrast image of the intact vesicle. After the injection starts (from the right side), small high-contrast domains form on the vesicle surface facing the micropipet. The snapshots at 42 and 43 s show the vesicle with the small domains visualized with phase-contrast (see arrows and magnification of one domain in the inset) and fluorescence microscopy. All GUVs kept their optical contrast after the formation of these domains. Eventually, the vesicle bursts through the opening of a large hole (108.45 s), which seems to have originated from the small domains, and releases its entrapped volume rapidly. We want to stress that the peptides did not induce vesicle adhesion to the coverslip and that vesicle burst was, therefore, a direct consequence of peptide−lipid interaction.

To gain further insight into the Gm lytic mechanism, injection of a fluorescent analogue, Gm-Rh, was also investigated. In this way, we could follow with fluorescence microscopy the fate of the Gm-Rh in a nonlabeled GUV. To the best of our knowledge, this is the first study with a fluorescently labeled AMP with optical

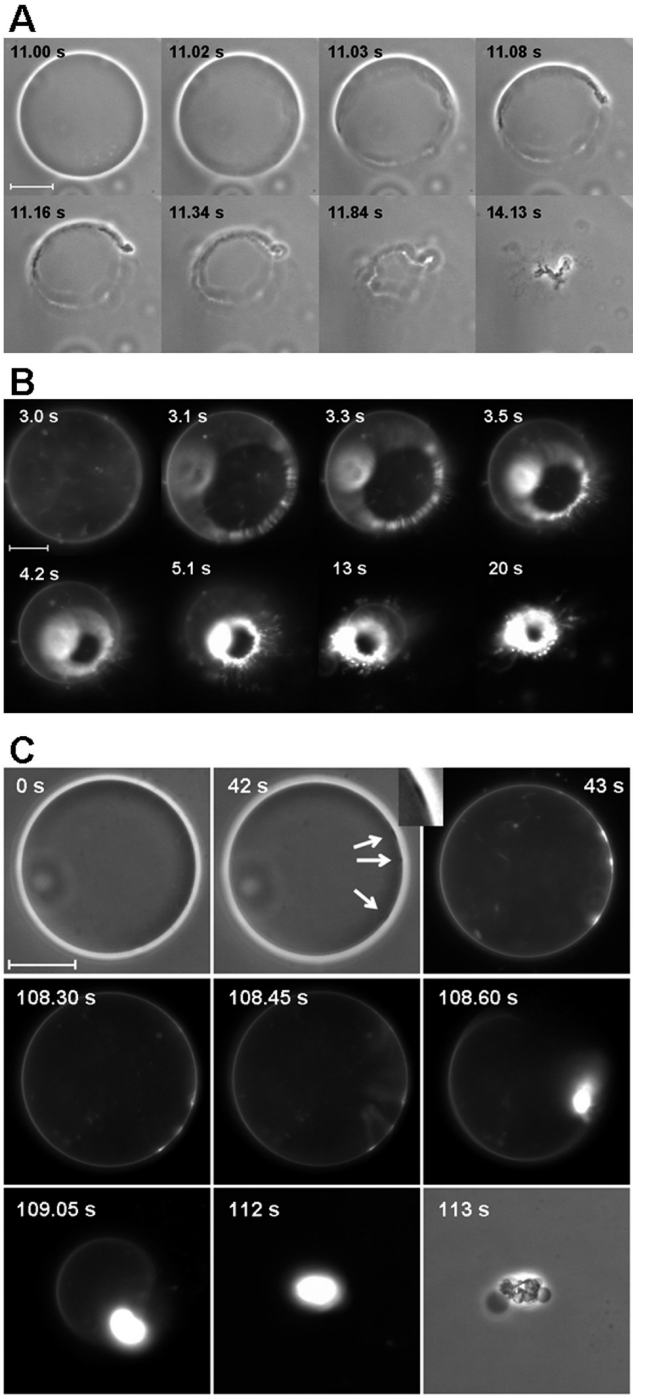

Figure 2. Sequences of phase-contrast and fluorescence microscopy images showing the burst of GUVs caused by micropipet injection of Gm from the right side. (A) Phase-contrast images of a POPC/POPG 1:1 GUV experiencing injection of a 100 μM Gm solution. (B) Fluorescence microscopy images of a POPC GUV containing 1 mol % $DiIC_{18}$ experiencing injection of a 50 μM Gm solution. (C) Phase-contrast (0, 42, 113 s and inset) and fluorescence microscopy images (43−112 s) of a GUV made of POPC containing 1 mol % $DiIC_{18}$ experiencing injection of a 50 μM Gm. The arrows point to small high-contrast domains formed on the GUV surface. The inset shows a magnification of the uppermost domain. The time shown on top of each sequence is relative to the moment when the micropipet was brought close to the vesicle. The scale bars in the first image of each sequence represent 20 μm.

(32) Dobereiner, H. G. *Curr. Opin Colloid Interface Sci.* **2000**, *5*, 256–263.
(33) Tanaka, T.; Tamba, Y.; Masum, S. M.; Yamashita, Y.; Yamazaki, M. *Biochim. Biophys. Acta* **2002**, *1564*, 173–182.
(34) Yamashita, Y.; Masum, S. M.; Tanaka, T.; Yamazaki, M. *Langmuir* **2002**, *18*, 9638–9641.
(35) Inaoka, Y.; Yamazaki, M. *Langmuir* **2007**, *23*, 720–728.
(36) Mally, M.; Majhenc, J.; Svetina, S.; Zeks, B. *Biochim. Biophys. Acta* **2007**, *1768*, 1179–1189.

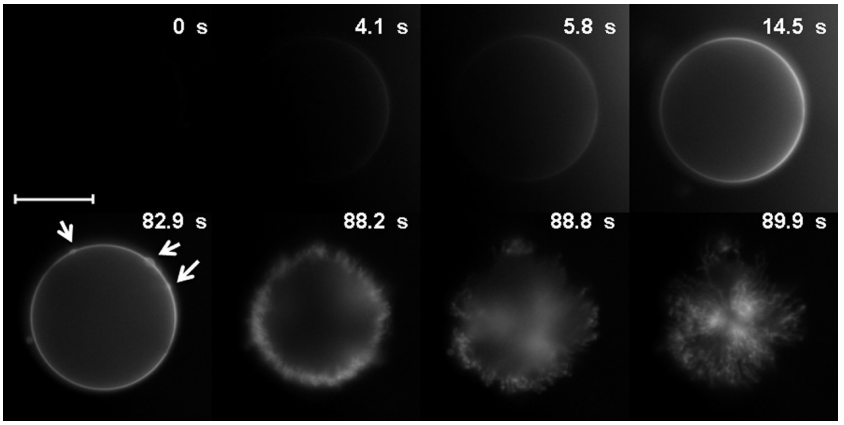

Figure 3. Sequence of fluorescence microscopy images showing the effect of injection of a fluorescently labeled peptide solution (50 μM Gm-Rh) close to a GUV made of POPC/POPG 1:1. The time shown on top is relative to the moment when the micropipet was brought close to the vesicle (from the right side). The arrows indicate the formation of dense regions. The scale bar represents 20 μm.

microscopy of giant vesicles. It is important to mention, however, that Gm-Rh performed worse than Gm in microbiology assays, indicating that the attachment of the fairly big rhodamine group altered to some extent peptide conformation and therefore antimicrobial activity. Nonetheless, from a qualitative point of view, both labeled and nonlabeled peptides acted in a similar way against GUVs, justifying the use of this analogue to obtain fluorescence microscopy images of the peptides. Figure 3 illustrates a typical injection of Gm-Rh close to a GUV. In the first image, the vesicle cannot be visualized because initially the GUV is not fluorescent. As the injection starts (from the right side), the membrane surface becomes faintly fluorescent after 4.1 s, indicating that Gm-Rh is binding to the lipid bilayer. At this point, the fluorescence intensity is higher on the side facing the micropipet. The fluorescence intensity at the vesicle surface increases as the injection continues, until at 14.5 s the surface of the membrane becomes completely covered with Gm-Rh, clearly showing the very high affinity of the positively charged Gm-Rh to the negatively charged GUV. In the next image, we can again observe high-contrast domains on the membrane surface (at 82.9 s, marked with arrows), which indicates a local accumulation of peptides. Thus, these regions consist of an accumulation of lipids (see Figure 2C) and peptides. The peptide/lipid assembly in such structures is unknown. Shortly after these domains appear on the vesicle surface, a large hole forms and the GUV suddenly bursts (at 88.2 s). The bilayer disintegrates into thin structures, which remain fluorescent (last snapshot, at 89.9 s). Interestingly, a similar membrane disintegration process was observed after application of a strong electric pulse on negatively charged GUVs.[37]

The visualization of the fluorescent peptide flux coming out of the micropipet allowed us to confirm that the peptide concentration (fluorescence intensity) close to the vesicle was much lower than the one loaded in the micropipet. Only when the injection flux became so strong that significant GUV drift occurred did the peptide concentration close to the vesicle reach similar values as inside the micropipet. Other studies with microinjection assume that the concentration close to the vesicle is the same as that inside the micropipet,[25,28,29] whereas others say that it should be a little lower.[33] In our setup, it was clear that the solution was rapidly diluted after injection, and a steady-state condition could only be achieved at lower peptide concentrations. In principle, the quantification of the fluorescence intensity at the GUV surface could be correlated with the local peptide concentration and used to estimate the peptide/lipid ratio causing vesicle destruction. However, due to the relatively fast photobleaching of the rhodamine label attached to the peptide and to the fact that the fluorescence image with conventional microscopy has also contributions from unfocused planes, this could not be achieved.

Evaluation of the Lytic Activity of Gm and GmL. In the previous section, we showed that Gm induces a sudden burst of the GUVs. Similar results were obtained for GmL (data not shown). However, the injection with micropipets did not allow a quantification of the lytic activity of the peptides. In this section, we show a protocol to measure the lytic activity of different concentrations of Gm and GmL against different membrane compositions. GUVs made of POPC with 0−55 mol % POPG or 40 mol % cholesterol were prepared in a sucrose solution and further diluted into a glucose solution containing different concentrations of peptide. Right after the dilution, the solution of GUVs was placed in an observation chamber under the microscope, and an optical field was chosen and recorded with a low magnification objective. In the absence of peptide, GUVs prepared with the sucrose/glucose asymmetry slowly deposit on the coverslip surface of the observation chamber due to gravity, as shown in Figure 4A. Soon after the chamber is placed on the microscope stage, few GUVs can be seen at the bottom of the chamber. After 15 min, the number of GUVs increases considerably. However, if the same procedure is done in the presence of a sufficiently high peptide concentration, the number of intact GUVs is significantly reduced, because of the induced vesicle bursting shown in the previous section. This is illustrated for one particular experiment in Figure 4B, in which GUVs made of POPC with 25 mol % POPG were diluted in a glucose solution containing 0.2 μM Gm. It is important to stress that the deposition of GUVs does not imply vesicle adhesion to the coverslip, as mild drift of vesicles was observed throughout the whole experiment, both in the absence and in the presence of peptides. Experiments as shown in Figure 4A and B were done for different Gm concentrations, and the number of intact GUVs (nonburst) was counted as a function of time. One typical set of data is shown in Figure 4C, in which the number of intact GUVs is plotted as a function of time for increasing Gm concentration. In the absence of Gm, the number of GUVs increases almost linearly with time. As the Gm concentration is increased, the inclination of the curve decreases until a horizontal line indicates when hardly any GUVs are observed throughout the whole experiment. Even though the absolute quantity of GUVs is dependent on the particular preparation and on the optical field chosen, it is clear that the slope of

(37) Riske, K. A.; Knorr, R. L.; Dimova, R. *Soft Mater* **2009**, *5*, 1983–1986.

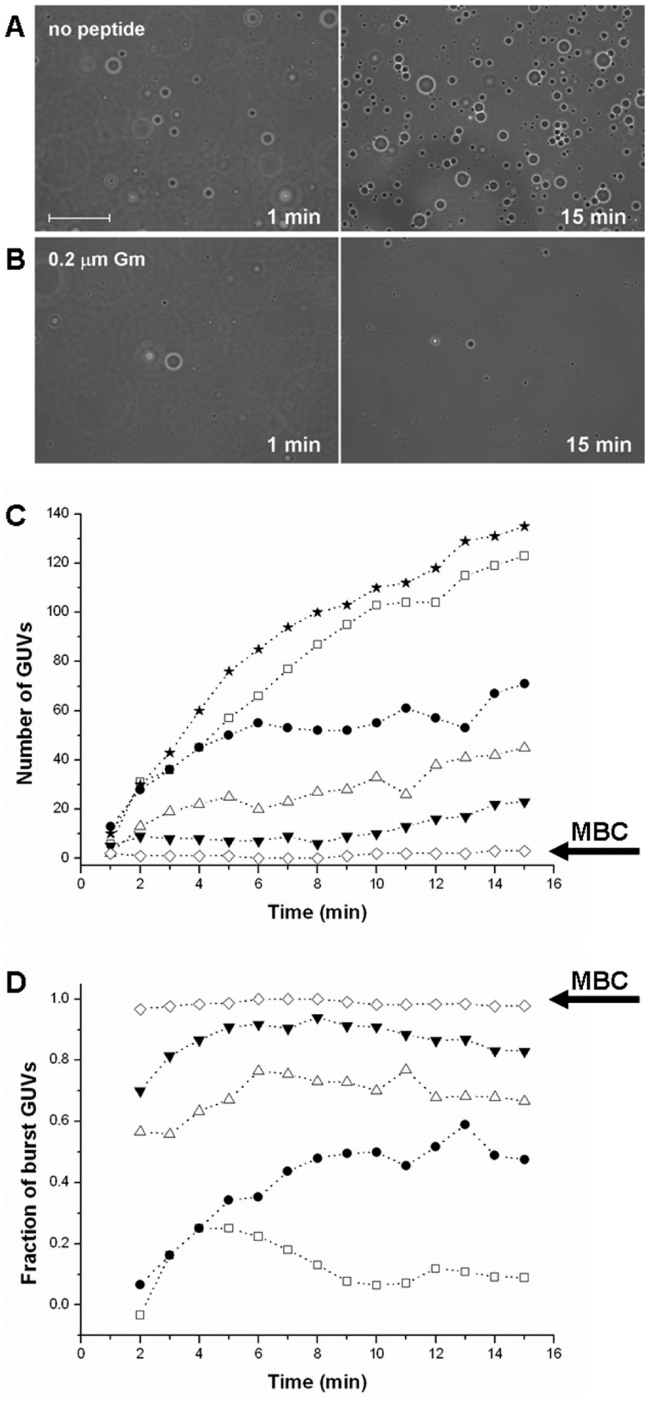

Figure 4. (A) Selected optical field captured with a low magnification objective (10× Ph1) showing the usual deposition of GUVs due to gravity. The picture on the left side shows this area 1 min after the solution was placed inside the observation chamber. The picture on the right side shows the same area after 15 min. (B) Similar to (A), but with GUVs diluted in a solution containing 0.2 μM Gm. The scale bar represents 200 μm. (C) Number of GUVs counted in a selected optical field as a function of time in the presence of different Gm concentrations, namely, (★) 0, (□) 0.05, (●) 0.07, (△) 0.10, (▼) 0.15, and (◇) 0.20 μM Gm. Only GUVs bigger than 5 μm were counted. (D) Fraction of burst GUVs calculated from the ratio of the number of GUVs in the presence and in the absence of Gm. The symbols are the same as in (C). Dotted lines connecting points are only a guide to the eyes. The arrows point to the MBC, the minimum bursting concentration, defined as the lowest peptide concentration causing extensive bursting (fraction of burst GUVs ~ 0.9) of the collection of GUVs. The GUVs were made of POPC with 25 mol % POPG.

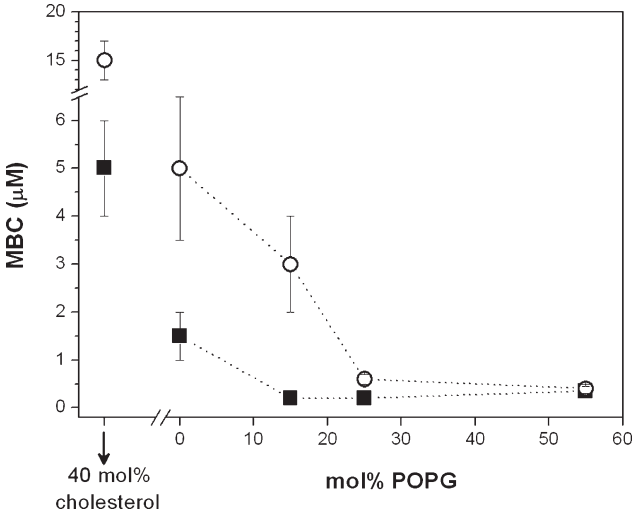

Figure 5. Minimum bursting concentration (MBC) of Gm (■) and GmL (○) against GUVs of different membrane composition. The MBC represents the lowest peptide concentration causing extensive bursting (~90%) of GUVs in a preparation, as illustrated in Figure 4C and D for one particular set of data. Dotted lines connecting points are only a guide to the eyes. The error bars refer to the average of two or three different set of experiments.

the curves is highly dependent on the Gm concentration. The fraction of burst GUVs can be estimated from the ratio between the number of intact GUVs in the presence and in the absence of peptide. This is shown in Figure 4D for this particular set of data. In this way, the temporal dependence of the deposition of GUVs is eliminated and the results only depend on the dynamics of the lytic activity of the peptide. We can see that equilibrium is reached after ~8 min for low Gm concentrations and much faster for higher Gm concentrations.

In order to evaluate the lytic effect of the peptide against a particular membrane composition, we defined a new parameter denoted by MBC (minimum bursting concentration), which corresponds to the lowest concentration of the peptide leading to extensive bursting of an ensemble of GUVs (defined as ~90% bursting). This parameter was inspired on the widely used MIC (minimum inhibitory concentration) from microbiology assays, which indicates the lowest concentration of an antimicrobial agent that inhibits the growth of a microorganism after incubation. As can be seen in Figure 4C and D, the MBC of Gm against POPC with 25 mol % POPG is 0.2 μM.

The same procedure shown in Figure 4 was carried out in order to obtain the MBC of both Gm and GmL against different membrane composition, namely, POPC with 0, 15, 25, and 55 mol % POPG and POPC with 40 mol % cholesterol. The values of the MBC found for both peptides are summarized in Figure 5 as a function of membrane composition. The error bars refer to the average of two or three different sets of experiments. Similar values of MBC were found for 25 and 55 mol % POPG in a buffered solution (1 mM HEPES pH 7.5 with 0.2 mM EDTA, results not shown).

For each peptide, it is clear that the MBC decreases as the fraction of the anionic lipid POPG in the membrane increases, implying that the lytic activity is enhanced by the membrane surface charge. These results clearly demonstrate the fundamental role played by electrostatic interaction between the cationic peptides and the anionic membranes. On the other hand, the lytic activity was considerably reduced against POPC with 40 mol % cholesterol, due to the well-known ordering effect of cholesterol in

membranes. Furthermore, cholesterol resides in the hydrophobic core of the bilayer, contributing with negative intrinsic curvature and therefore acting against pore formation.

As expected, Gm showed to be more effective than GmL. The difference in lytic activities was more pronounced in the absence of surface charges and decreased as the molar fraction of POPG in the membrane increased. It is important to recall that both peptides bear the same net charge ($z = +6$) and hydrophobicity. Therefore, the difference in activity should arise from the different structures adopted by the peptides, and consequently in their binding affinity to the membrane. The MBC against pure POPC vesicles was $1.5 \pm 0.5\ \mu$M Gm and $5.0 \pm 1.5\ \mu$M GmL. Addition of 15 mol % POPG to the membrane already caused an almost 10-fold decrease in the MBC of Gm, to $0.2 \pm 0.1\ \mu$M. Surprisingly, this value remained relatively constant for higher POPG molar fraction and was even slightly higher for 55 mol % POPG, $0.35 \pm 0.1\ \mu$M Gm. On the other hand, as the molar fraction of POPG in the membrane was increased, the MBC of GmL decreased gradually, although not linearly, reaching eventually a similar lytic activity as Gm at the highest POPG molar fraction. The existence of this maximum activity plateau around MBC = $0.2\ \mu$M peptide corresponds probably to complete covering of the charged lipid bilayer with peptides. An estimate of the peptide-to-lipid ratio associated with the MBCs shown in Figure 5 can be given, although rough, because the lipid concentration from GUVs is quite low and therefore difficult to measure. Previous results suggest that the lipid concentration is around 1 μM. Thus, the MBC values shown in Figure 5 should correspond to peptide-to-lipid ratios ranging from 15 (for the GUVs containing cholesterol) to 0.2 (obtained at high POPG fraction) peptides/lipid.

We can now correlate the lytic activity measured with the dilution protocol with the one induced by injection with a micropipet loaded with a peptide solution. For high POPG content, the MBC lies around $0.3\ \mu$M (see Figure 5), whereas for POPC it is much higher, $1.5\ \mu$M Gm. However, visible lytic effects on POPC/POPG GUVs experiencing a Gm flow from the micropipet were only observed when the peptide concentration inside the micropipet was at least $10\ \mu$M. Similarly, $50\ \mu$M Gm was needed to induce lytic effects on POPC GUVs. This shows once again that the peptide concentration close to the GUVs in the injection protocol is typically 10−30 times lower than that of the original solution.

Interestingly, the MBC values found for Gm and GmL against GUVs composed of POPC/POPG mixtures were similar to the MIC values obtained for the same peptides against the microorganisms *C. albicans* and *E. coli*, which were performed also at low ionic strength (~0.3−0.6 μM Gm and ~10 μM GmL, ref 12). This indicates that the interaction with the lipid bilayer is certainly crucial for the antimicrobial activity of these peptides. Additionally, the lytic assay with GUVs is relevant in predicting antimicrobial activity in vivo.

We can conclude that the lytic activities of both peptides against GUVs depend on two major factors, as expected: peptide concentration and membrane surface charge. Recently, Tamba and Yamazaki[25] showed a similar trend for magainin 2 interacting with membranes of PC/PG at different ratios. They showed that antimicrobial activity was dependent on the surface concentration of peptide only, which increases with surface charge density. However, a saturation effect with increase in PG fraction such as that exhibited by Gm was not observed. It should be stressed that the ionic strength in our protocol is much lower than that used by Tamba and Yamazaki.[25] Furthermore, the partition coefficients of both Gm and GmL are not yet known. Therefore, our results cannot be expressed as a function of peptide concentration at the bilayer surface, as done in ref 25. Studies with isothermal titration calorimetry are currently being performed, so that the binding affinities of both peptides can be determined.

Discussion

The optical microscopy data shown here clearly confirm that the lytic activity of both antimicrobial peptides studied, Gm and its linear analogue GmL, is higher against negatively charged bilayers and lower against bilayers with cholesterol. Thus, surface charge and membrane fluidity and/or intrinsic curvature are important parameters to the interaction of these peptides with membranes, and might be of importance for their antimicrobial activity in vivo, since the membrane of microorganisms contains a high fraction of charged lipids, whereas the plasma membrane of erythrocytes contains a high fraction of cholesterol.

Injection of Gm and GmL close to GUVs revealed that both peptides exhibit a similar lytic mechanism, irrespective of the membrane composition. Initially, the peptides adsorb onto the external leaflet, causing an increase in the lateral pressure of the external monolayer, seen by an increase in the spontaneous curvature of the vesicles. This step could only be visualized in vesicles that had some excess area allowing for shape changes. At this stage, a shallow penetration of the hydrophobic residues might occur. However, the membrane integrity is maintained, since the GUVs retain the original sugar asymmetry across the bilayer. Later, the GUVs burst suddenly in a stochastic way, releasing their inner content rapidly. A leaky vesicle with stable pores was not observed, irrespective of the peptide concentration. According to studies on the interaction of other AMPs with GUVs, vesicle burst is a clear indication of lytic activity via the carpet model.[28,30] On the other hand, peptides which form stable toroidal pores increase the membrane permeability to small molecules without destroying the vesicle.[27,29,30] We thus propose that both Gm and GmL act via the carpet model. Generally, GUVs disintegrated into interconnected thin structures. This observation might indicate the preference for highly curved structures for high peptide/lipid ratios. Interestingly, the antimicrobial peptide temporin B induced tubular growth on supported lipid bilayers containing POPG.[38] The authors discuss their results in light of the positive curvature stress induced by the peptide.

Vesicle burst due to action of Gm and GmL was often preceded by the formation of small high-contrast domains on the vesicle surface, seen in phase-contrast mode and with fluorescence microscopy of both membrane probes and fluorescent peptides. Therefore, these regions contain high accumulation of peptides and lipids, although their exact structure remains unknown. Such regions were also observed during the lytic action of other AMPs which act via the carpet model, such as the tea catechin EGCg.[28] Conversely, such regions were not reported when AMPs which form toroidal pores were investigated. We speculate that these defects might trigger vesicle burst, as suggested by Lee et al.[27]

Gm adopts a quite stable β-hairpin structure conferred by the two disulfide bridges formed between its four Cys residues.[15] Previous studies revealed the amphipathic character of this β-hairpin structure: the hydrophobic residues Tyr^7, Val^{12}, Leu^5, and Tyr^{14} face one side, whereas the cationic residues $Arg^{3,4,10,16,18}$ and Lys^8 face the other side. Thus, it seems reasonable to propose that initially the cationic residues interact with the negative phosphates at the membrane surface with a shallow penetration

(38) Domanov, Y. A.; Kinnunen, P. K. J. *Biophys. J.* **2006**, *91*, 4427–4439.

of the hydrophobic residues. This increases the stress on the bilayer, and at a threshold peptide/lipid ratio the membrane is destabilized.[39] Several authors pointed out the importance of the hydrophobic match in the lytic mechanism of AMPs.[30,40] Only peptides long enough to span the bilayer core (~30 Å) would be able to form a stable toroidal pore; short peptides would then act via the carpet model and disrupt the vesicle.[30] The length of Gm around 27 Å, with a relatively short hydrophobic patch of ca. 7 Å (estimated from ref 15), would not suffice to span the whole bilayer core. Therefore, this hydrophobic mismatch would also be consistent with a lytic action via the carpet model.

The linear analogue GmL has the original four Cys residues of Gm replaced by Ser, and therefore, it adopts a random structure in aqueous solution, since no disulfide bridges exist to impose the kink of the β-hairpin structure. However, previous circular dichroism (CD) results showed that this peptide has a tendency to adopt some structuring in the presence of SDS micelles, with features similar to those exhibited by Gm.[14] The same structuring is expected once this peptide accumulates at a bilayer interface. As a result, the interaction of GmL with the membrane is rather similar to that of Gm, even though its lytic activity is lower. From our results (see Figure 5), we showed that the lytic activity of GmL, as compared to Gm, is much lower against neutral bilayers and increases for higher fractions of POPG. At high surface charge density, the lytic activity of both peptides is similar. Therefore, it seems that the presence of membrane surface charges plays a key role on the structuring of the GmL analogue. The interaction between the cationic residues and the phosphate groups of POPG could induce the bending of the peptide chain, which would then acquire a conformation resembling the amphipathic β-hairpin structure of Gm.

The structural motif of Gm is shared by other antimicrobial peptides, such as protegrin-1 and androctonin.[15] Hence, it is believed that their mode of action might also be similar. However, it should be noted that the hydrophobic/hydrophilic character of the AMP is fundamental to the peptide/membrane interaction. The hydrophobic profile of Gm resembles that of protegrin-1, although the hydrophobic patch of the latter is larger than that of Gm.[15] Previous works with protegrin-1 showed that its activity is also enhanced in the presence of POPG and suppressed in the presence of cholesterol.[41] Furthermore, NMR data showed that protegrin-1 was able to fragment POPG-containing vesicles, indicating that its lytic activity is similar to that of Gm.[41] Another study stressed the importance of the lipid length on the effect caused by protegrin-1:[42] the peptide disrupted vesicles of the long lipid POPC but was able to insert into bilayers of the short lipid DLPC (dilauryl phosphatidylcholine, with 12C only) without destroying the vesicles. Likewise, studies on another AMP, the cyclic β-hairpin peptide retrocyclin-2, revealed that this peptide was able to adopt a transbilayer conformation in DLPC bilayers, whereas it laid with an almost parallel alignment in POPC membranes.[40] These studies show the importance of the hydrophobic match discussed here and elsewhere.[30,40]

Conclusion

Using the single GUV method, we showed that micromolar concentrations of the antimicrobial peptide Gm and its linear analogue GmL induce burst of GUVs made of mixtures of POPC and POPG, resulting in the rapid leakage of the vesicle internal content and vesicle collapse into unresolved tubular structures. Moreover, formation of stable pores in the GUVs was not observed. These facts lead us to propose that both Gm and GmL disrupt the membrane via the carpet model. The lytic activity of both peptides is enhanced by the presence of the anionic phospholipid POPG and decreased upon addition of cholesterol. Therefore, membrane surface charge density and fluidity and/or intrinsic curvature play an important role in lytic activity. Our results show that Gm is more active than its linear analogue GmL, as expected, but the difference in activity decreases as the POPG content in the membrane increases. This indicates that surface charges might play a key role in inducing a more active conformation to GmL.

Gm is known to inhibit growth of both Gram-positive and Gram-negative bacteria when added into the bacterial culture medium and to have significant hemolytic activity. Our results show that Gm induces burst of GUVs of both model membrane systems used, POPC/POPG mixtures mimicking bacterial membranes and POPC/cholesterol resembling the membrane composition of erythrocytes, although with different efficiency. Albeit the targets for antimicrobial activity in vivo might comprise, for instance, direct interactions with membrane proteins and polysaccharides, it seems clear that the interaction of Gm with the lipid phase is crucial to its lytic activity. Moreover, we want to stress the relevance of in vitro studies with GUVs. The MBC values obtained with the GUV assay presented here are in good agreement with the antimicrobial activities (MIC values) obtained from the microbiology assays. Consequently, studies with GUVs provide an easy way of testing the potential antimicrobial activities of several lead compounds.

Acknowledgment. We are thankful to M. T. Lamy for allowing us to prepare our samples in her lab, to the Department of Applied Physics (IF-USP) for the infrastructure facilities, to J. Aboulafia and V. L. A. Nouailhetas for the use of the micropipet puller, to S. Daffre for the biological results, and to R. Dimova for proofreading the text. This work was supported by FAPESP, CNPq, and FADA/UNIFESP. A.M. and T.M.D. are recipients of CNPq fellowships. K.A.R. acknowledges the financial support of inctFCx.

(39) Huang, H. W.; Chen, F. Y.; Lee, M. T. *Phys. Rev. Lett.* **2004**, *92*, 198304.
(40) Tang, M.; Waring, A. J.; Lehrer, R. I.; Hong, M. *Biophys. J.* **2006**, *90*, 3616–3624.
(41) Mani, R.; Buffy, J. J.; Waring, A. J.; Lehrer, R. I.; Hong, M. *Biochemistry* **2004**, *43*, 13839–13848.
(42) Marasinghe, P. A.; Buffy, J. J.; Schmidt-Rohr, K.; Hong, M. *J. Phys. Chem. B* **2005**, *109*, 22036–22044.